3 Preprocessing of the data sets

Coherent and incoherent noise strongly influence the processing of seismic data and thus the quality of the resulting images. This noise can appear as a result of many different physical processes. The attenuation of the different noise types is one of the most complex problems in seismic data processing since useful information of the underlying data has to be preserved. While the origin of unpredictable incoherent (or random) noise is hard to detect and to remove, strategies to attenuate specific modes of coherent noise such as multiples are well known. Two of these latter methods will be introduced and discussed in the following sections after a short description of the data sets.

3.1 The data sets

The seismic data sets used in this study were kindly provided by the Federal Institute for Geosciences and Natural Resources (Bundesanstalt für Geowissenschaften und Rohstoffe (BGR)). Within this thesis, the entire line SO104-13, acquired in the southern region of the investigation area, was processed but only a 120 km long section of line SO104-07 (cf. Figure 2.3). This is exactly the part crossing the trench whereas the complete profile length was about 430 km most of it located seaward of the trench up to approximately 75°W.

3.1.1 Acquisition parameters and characteristics of the data

During the recording period, two airgun arrays on both sides of the research vessel "Sonne" were used and, depending on the sailing speed, the shots were triggered in time intervals of 18 s resulting in a shot spacing of approximately 50 m. To avoid ghost multiples between water surface and receivers, the streamer was positioned at a depth of about 9 m. The latter contained seismic instruments as well as units to interactively control the streamer depth. A full description of the equipment and a complete list of all parameters is given in Hinz *et al.* (1995).

For both profiles the acquisition parameters are similar. The maximum offset was about 3 km with an equidistant channel interval of 25 m. This results in an average CMP-fold of 28. The recording time was somewhat more than 14 s and the sampling rate was 4 ms. All of the 2246 shots on line SO04-13 were used but only 2310 of a total of 8580 shot records on line SO104-07. Both data sets were bandpass filtered using a Butterworth filter with a low-cut frequency of 5 Hz and a high-cut frequency of 64 Hz.

3.1.2 Data quality

The quality of the data is extremely different for both areas of interest. In Figure 3.1 two representative shot gathers illustrate this difference.

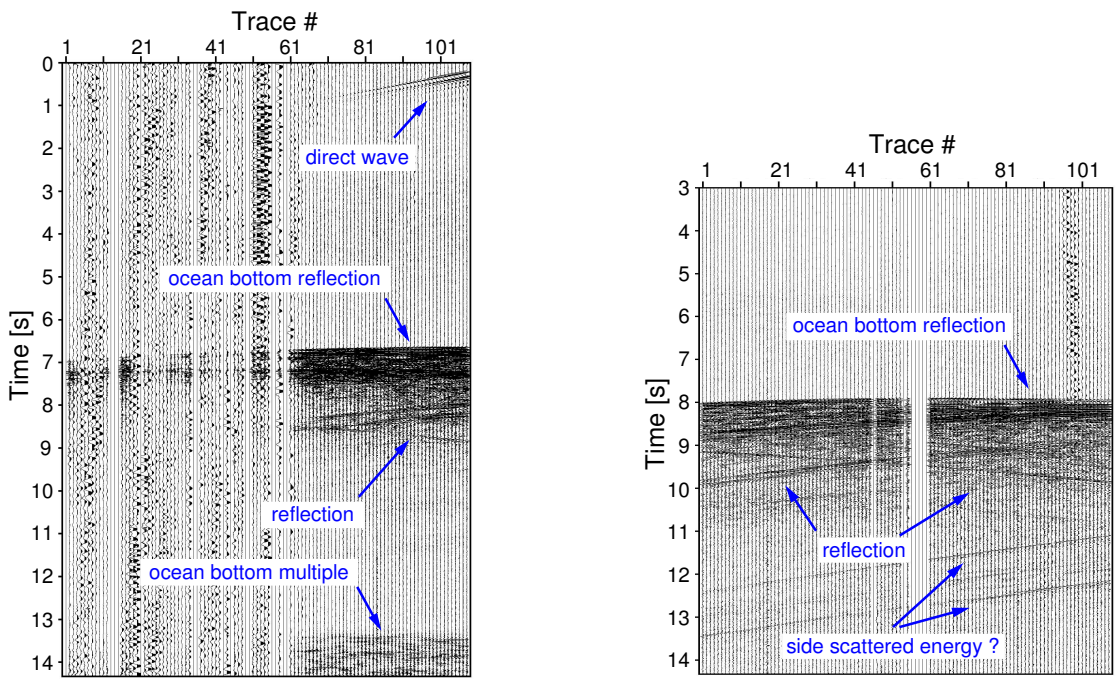

(a) Raw data common shot gather from line SO104-07.

(b) Raw data common shot gather from line SO104-13.

Figure 3.1: Illustration of the data quality by means of two representative shot gathers from line (a) SO104-07 and (b) SO104-13.

Within both shot gathers, the main reflection events are labelled: the direct wave between 0 s and 1 s in Figure 3.1(a); the ocean bottom reflection at 7 s (Figure 3.1(a)) and 8 s (Figure 3.1(b)); and the ocean bottom multiple in the shot gather of line SO104-07 (Figure 3.1(b)) at about 13 s. Note that the first 3 s of data set SO104-13 were removed to reduce the amount of data. Except for events

which were interpreted as possible side scattered energy (between 11 s and 13.5 s in Figure 3.1(b)) arising below such shot points where the ocean bottom has a strongly pronounced relief, SO104-13 is a high quality data set. In contrast, the recordings from line SO104-07 are, in parts, unsatisfying especially at both ends of the profile. Thereby, mainly the first few traces (far offset traces) are affected by strong noise (Figure 3.1(a)) maybe due to technical problems during acquisition. In comparably shallow water regions (east and west of the trench) later arriving signals are disturbed by the ocean bottom multiple. Different dipping reflections between 8 s and 13 s two-way-travel time in Figure 3.1(b) also arise in shot gathers from areas where the ocean bottom exhibits a pronounced topography (cf. Figure 2.1).

3.1.3 Basic preprocessing steps

Due to the relatively bad data quality of line SO104-07, a manually performed trace editing was necessary. Channels which were corrupt in all shots gathers were excluded. A top mute was applied to remove noisy signal from above the seafloor including the direct wave (Figure 3.1(a)).

Prior to the suppression of the ocean bottom multiples, a normal moveout correction (NMO) of the primary ocean bottom reflection had to be carried out. This procedure required reliable information about the velocity of the first arrivals which is, in the case of marine data, the water velocity. A semblance analysis was performed to determine the exact values. The result of this analysis is shown in Figure 3.2.

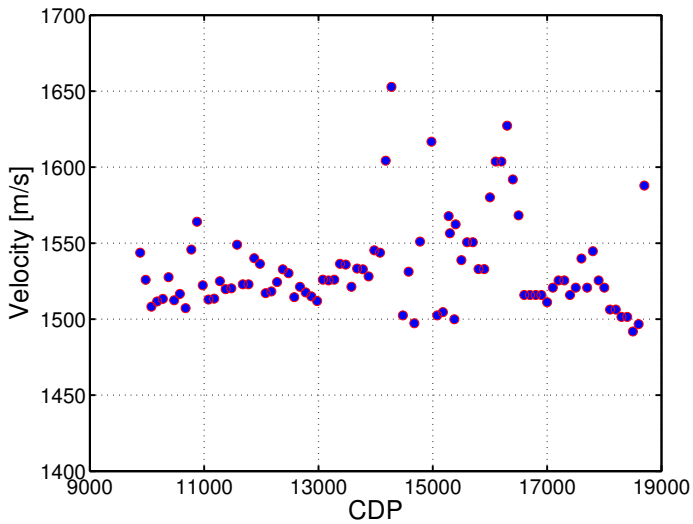

Figure 3.2: Picked velocity values of the primary ocean bottom reflection. Nearly all values are distributed around the mean value of about 1515 m/s except for that section of the profile located between CDP 14000 and CDP 16000.

Here, the water velocity is plotted over the CDP. Almost all values are distributed between 1500 m/s and 1530 m/s with a mean value of approximately 1515 m/s. Between CDP 14000 and 16000 a precise velocity determination was impossible due to the rough seafloor near the trench (Figure 2.1), i.e. the data include reflections arriving from variously dipping surface structures near the shot position. However, the outliers observed in this CDP range were insignificant for the objectives of this study. The water depth and the short recording time ensured that no ocean bottom multiples were recorded. The picked values apart from the trench region were then used for NMO correction.

3.2 Applied filtering techniques

In addition to incoherent noise, recorded seismic signals naturally consist of various superimposed wave types such as refracted waves (head waves), multiples or side scattered energy (e.g. from the rough surface of the ocean bottom, see for example Larner *et al.*, 1983; Coltrin & Backus, 1989; Gragg *et al.*, 2001). Due to the different characteristics, the suppression of each type requires an individual strategy. Within this thesis, the main focus was put on both the multiples (since they strongly disturb the resulting images in the subsurface) and on events that might be side scattered energy (which produce strong migration smiles in some areas along the profiles).

The application of a parabolic Radon filter to the data attenuated most of the multiple energy, whereas other unwanted coherent signals (for example head waves travelling along the sedimentary layers) were eliminated by using a frequency-wavenumber filter. Both techniques work with decomposition of multichannel seismic data into their plane wave components (e.g. Müller, 1971; Treitel *et al.*, 1982; Milkereit, 1987b).

3.2.1 Ocean bottom multiples attenuation

Besides other techniques for multiple suppression, such as f-k (frequency-wavenumber) multiple attenuation (e.g. March & Bailey, 1983; Zhou & Greenhalgh, 1994b) or methods based on deconvolution (e.g. Taner *et al.*, 1995), Radon filtering provides a practicable tool to remove multiples from the input seismic data especially in cases where the primaries and the multiples overlap in the f-k space (e.g. Zhou & Greenhalgh, 1994b). This type of filter uses the Radon transform (Radon, 1917; Chapman, 1981) where the data are transformed from the time-offset $(t - x)$ domain into the intercept-ray parameter $(\tau - p)$ domain. The classical linear $\tau - p$ transform can be

written as follows (e.g. Zhou & Greenhalgh, 1994a)

$$v(p,\tau) = \int_{-\infty}^{\infty} u(x, t = \tau + px)\, dx\,, \tag{3.1}$$

where $v(p,\tau)$ is the so called *slant stack* section of the input wavefield $u(x,t)$, and p is the slowness or ray parameter. During this procedure, the data are stacked over offset x along straight lines of constant $t = \tau + px$. Foster & Mosher (1992) generalized equation (3.1) for arbitrarily curved lines by replacing x with an offset dependent function which performs stacking over hyperbolic surfaces arising in common shot gathers. Due to computational problems with the hyperbolic approximation, Hampson (1986) introduced a parabolic form of equation (3.1) useful for NMO corrected data in which multiples have a parabolic form. Thereby, the term p is no longer the slowness but the time difference between zero-offset time and far-offset time (*moveout*) for a given parabola (e.g. Hampson, 1986). Nowadays, this technique is one of the most commonly used forms of multiple attenuation.

Before the filter was applied, the input gathers had to be rearranged to CDP-gathers for NMO correction of the primary ocean bottom reflection. To estimate the most reasonable range of moveout values, used as input parameters for the filtering process, a few tests were carried out. In principle, the actual filtering works in the following way: An inner trace mute is performed in the $\tau - p$ domain (time-moveout

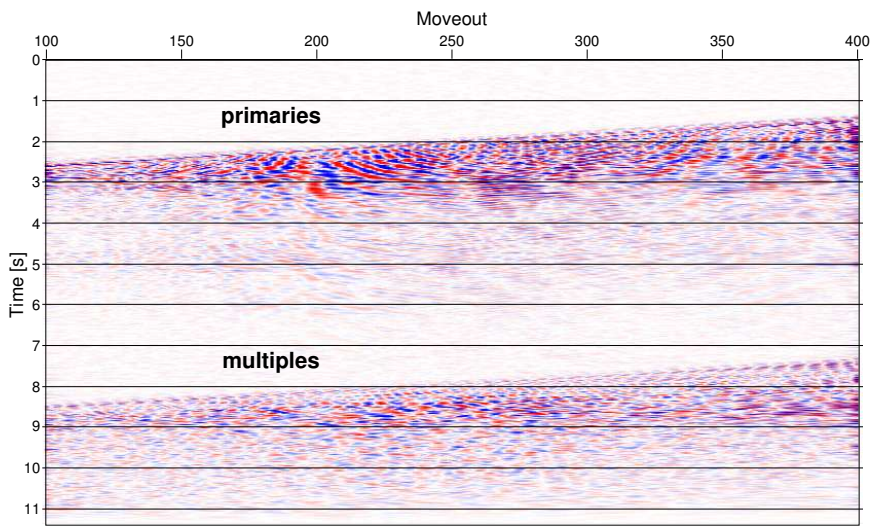

Figure 3.3: Time-moveout section of CDP 10150. The procedure is able to reliably distinguish between primary events and multiples. Within this $\tau - p$ section a top mute was applied so that only the part of the section remains which contain the multiples. These multiples are then modelled and subtracted from the input data.

domain, Figure 3.3) at which the primaries are removed and only the multiples are allowed to pass. These multiples are then modelled and subtracted from the input CDP-gathers. After filtering an inverse NMO is executed and the CDP data are re-sorted to common shot gathers.

Figure 3.4 shows an example for one shot of line SO104-13 before and after filtering. The ocean bottom multiple is clearly visible in Figure 3.4(a) at about 12 s two-way-travel time. In contrast, in the filtered shot gather (Figure 3.4(b)) this multiple is significantly suppressed. Here, it is obvious that near offset traces still contain some amount of multiple energy whereas for far offsets the multiples are almost completely removed. This effect, where parts of the near offset multiples are reintroduced to the seismic profile, is typical for parabolic Radon filtering (e.g. Marfurt *et al.*, 1996; Wang, 2003). However, most of the remaining multiple energy vanishes during migration so that this form of multiple attenuation leads to satisfactory results. A detailed discussion of the effect of filtering in the time-moveout domain to the amplitudes of the first arrivals, when the temporal distance between primaries and multiples is small, can be found in Kabir & Marfurt (1999).

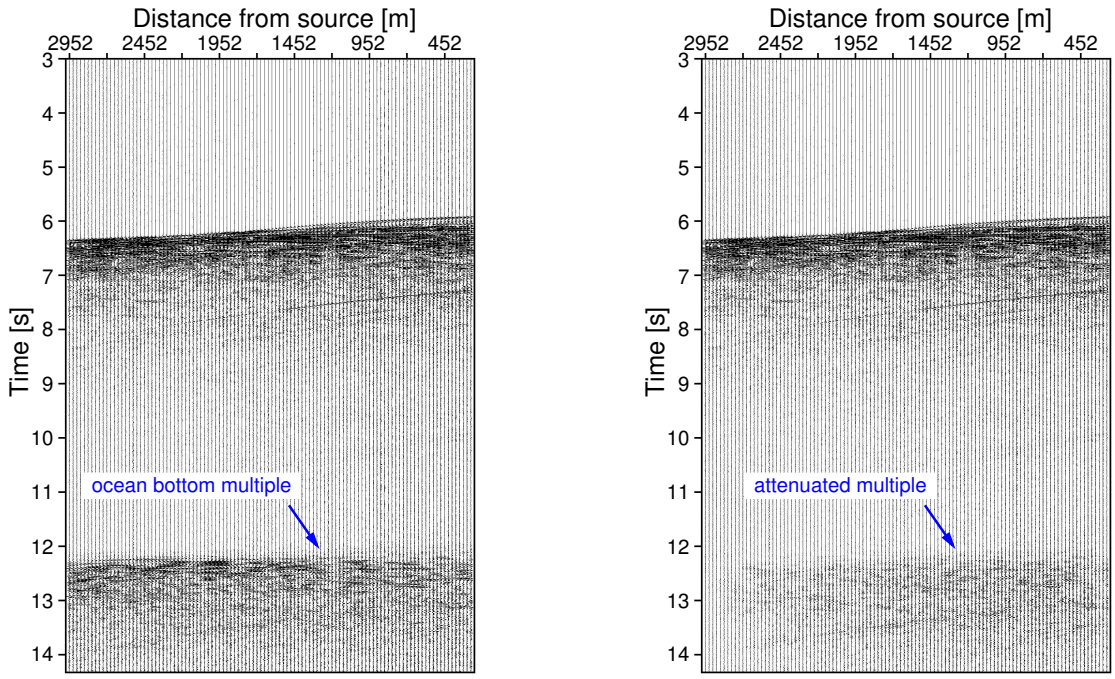

(a) Raw data common shot gather. *(b) Radon filtered common shot gather.*

Figure 3.4: Common shot gathers from data set SO104-13. (a) Raw data and (b) after Radon filtering. The ocean bottom multiple maps at about 12 s.

3.2.2 Filtering in the frequency-wavenumber domain

The various wave types differ not only in their frequency content but they also arrive with different apparent velocities. Frequency-wavenumber (f-k) filtering is generally used for the suppression of refracted waves, ground roll (e.g. Buttkus, 1991; Yilmaz, 2001) and, in some cases, for multiple attenuation (e.g. Zhou & Greenhalgh, 1994b) since all of these wave types should usually be isolated from the primary reflected energy in the f-k space. A 2D Fourier transform from time-offset domain to the frequency-wavenumber domain is the basic for this analysis (Bracewell, 1986). While head waves map as straight lines to the f-k domain, reflected energy is visible as a more or less triangular area around $k = 0$ (Figure 3.5). An approach to let pass this desired energy and to reject events mapping outside this area is given by a so-called *fan filter* (Treitel *et al.*, 1967). The frequency f and the wavenumber k are related via

$$f = v_a k, \tag{3.2}$$

where v_a is the apparent velocity which is the phase velocity of a wavefront travelling along a line of receivers (e.g. Sengbush & Foster, 1968; Sheriff, 1991). This means that the slopes of the lines through the origin in the f-k space indicate the apparent velocity.

A schematical diagram of the separation of wave types in the frequency-wavenumber domain is illustrated in Figure 3.5. The blue region around the frequency axis shows the area where primary reflected energy usually appears. Points outside of this triangle are related to different wave types associated e.g. with ground-roll (green area) or with backscattered noise (red).

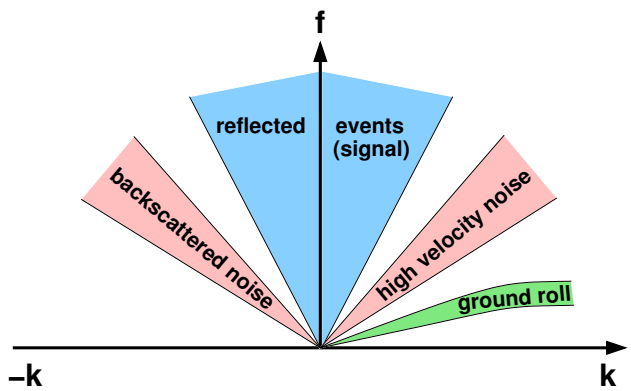

Figure 3.5: Principal mapping of different events in the f-k domain. The reflected energy surrounds the center ($k = 0$) (blue colored triangle), whereas noisy signal, as for example ground roll (green area) or backscattered noise (red area), is clearly separated from the center.

An example for a typical f-k plot calculated for a single shot gather of line SO104-13 is shown in Figure 3.6(a). In the negative wavenumber sector, outside the triangular center area, a region can be observed which can not be associated with reflected energy. It maps from the origin to a wavenumber of about $k = -0.02\ m^{-1}$ at a frequency of 50 Hz. These unwanted signals, arriving with negative apparent velocities (negative slope within the f-k domain) at the receivers, indicate a high content of backscattered energy in the data (cf. Figure 3.5). They are inhibited by using a fan filter where only the reflected energy around the center ($k = 0$) passes (Figure 3.6(b)). The effect of f-k filtering on the migration results will be discussed in chapter 5.

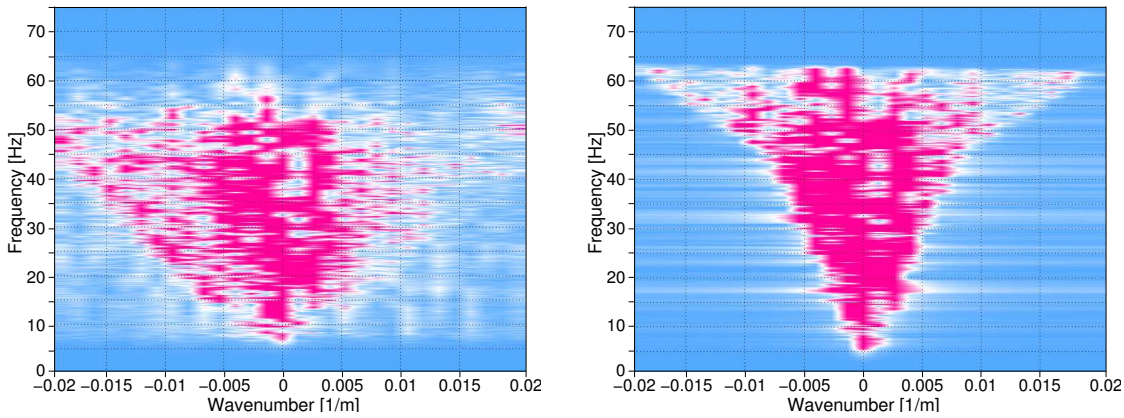

(a) F-k spectrum of a common shot gather from line SO104-07.

(b) Spectrum of the filtered shot gather.

Figure 3.6: (a) F-k spectrum of the raw shot gather 964 from line SO104-13. Backscattered energy maps in the negative k-sector and is suppressed by a fan filter (Figure 3.6(b)).